

Bureau International des Poids et Mesures

Guide on Secondary Thermometry

Specialized Fixed Points above 0 °C



Consultative Committee for Thermometry
under the auspices of the
International Committee for Weights and Measures

Specialized Fixed Points above 0 °C

CONTENTS

- 1 Introduction
- 2 Phase transitions as temperature references
 - 2.1 Unary or single-component fixed points
 - 2.2 Binary fixed points
 - 2.2.1 Eutectics
 - 2.2.2 Peritectics
 - 2.2.3 Eutectoids
- 3 Composition and temperatures for recently-investigated fixed points
 - 3.1 Liquid-vapour transitions
 - 3.2 Triple points
 - 3.3 Binary-metal systems
 - 3.4 Metal-carbon systems
- 4 Techniques for the calibration of contact thermometers
 - 4.1 Sealed cells
 - 4.2 Wire-bridge and coil methods for thermocouples
 - 4.3 Miniature cells
 - 4.4 Freezing points of nickel and palladium in alumina crucibles
 - 4.5 Metal-carbon fixed-point cells for thermocouples
- 5 The ice point (0 °C)
 - 5.1 The free-draining method
 - 5.2 The slush method
- 6 References

Guide on Secondary Thermometry

Specialized Fixed Points above 0 °C

F Edler, Physikalisch Technische Bundesanstalt, Germany
Y G Kim, Korea Research Institute of Standards and Science, Korea
G Machin, National Physical Laboratory, United Kingdom
J Pearce, National Physical Laboratory, United Kingdom
D R White, Measurement Standards Laboratory of New Zealand, New Zealand

ABSTRACT

The Guides on Secondary Thermometry are prepared by the Consultative Committee for Thermometry to provide advice on good thermometry practice and making temperature measurements traceable to the International Temperature Scale of 1990. This guide collates information on specialized fixed points and unconventional ways of realizing conventional fixed points, for fixed points above 0 °C. The information includes; a tutorial discussion on the nature of the different phase transitions exploited in thermometry; a summary of the composition, temperatures, and attainable accuracies for recently investigated phase transitions; and the principles of operation and typical performance characteristics for a range of different methods by which the fixed points can be realised. The document concludes with detailed advice on the realisation of the ice point (0 °C), because of its importance to contact thermometry.

1. Introduction

The International Temperature Scale of 1990 (ITS-90) defines the temperatures of a number of fixed points: the melting, freezing, and triple points of pure substances [Preston-Thomas 1990]. The fixed points are used as calibration points for standard thermometers, also defined by ITS-90. The fixed points should be realised in accordance with the ITS-90 and the recommendations of the *Guide to the Realization of the ITS-90* [Fellmuth *et al* 2015, Pearce *et al* 2015, McEvoy *et al* 2015]. These fixed points may also be used for the calibration of secondary thermometers.

The ITS-90 fixed points provide the highest level of accuracy available, but are not always at convenient temperatures, or realisable under the physical constraints of a particular measurement setup, or available with more modest uncertainties at a lower cost. Therefore, the purpose of this document is to provide guidance for the selection and realisation of fixed points in addition to those defined by ITS-90, and fixed points realised in conditions departing from the ITS-90 recommendations. The guide focuses on fixed points at or above 0 °C.

The following sections include a tutorial introduction to the phase transitions used for temperature references, the compositions and temperatures for a range of secondary reference points, the construction of specialised fixed points for contact thermometers, including miniature cells, sealed cells, and wire-bridges and coils. Finally, because of its importance to thermometry, the final section describes the realisation of the ice point.

Because of the large number of secondary reference points, this document is necessarily tutorial and is primarily a guide for the selection of fixed points rather than guidance for practical realisations. Where uncertainties are given, these are generally the standard uncertainties ($k = 1$) reported by the authors of the referenced papers, and are indicative rather than authoritative. For detailed advice, users should consult the references specific to the selected fixed point. Similarly, both the selection and practical realisation of fixed points are the subject of ongoing research, and users should consult more recent literature, if available, for further information.

2. Phase transitions as temperature references

A phase transition occurs when a system changes from one thermodynamic state, in which the matter has uniform physical properties, to another thermodynamic state. During the transition, one or more of the system properties change discontinuously because of changes in external conditions. For example, when a solid becomes liquid on a change of temperature, the properties that change discontinuously include the volume, density, enthalpy, and entropy.

Of particular interest for thermometry are first-order phase transitions, which exhibit a discontinuous change in enthalpy so that the system absorbs or releases

latent heat. The absorption or release of latent heat is used to maintain a fixed temperature.

Second- and higher-order phase transitions are also used in thermometry, but they require a separate measurement system to detect the change in the physical property of interest. For example, a separate resistance measurement system is required to determine when a superconducting transition takes place. To date, high-order phase transitions have been exploited only at cryogenic temperatures. More detailed information on the thermodynamics of phase transitions can be found in chemistry and thermodynamics texts. Much of the material presented in the following subsections is based on Prince [1966]. Naumann [2009] also contains helpful tutorial material on phase equilibria.

2.1. Unary or single-component fixed points

Figure 1 shows the pressure-temperature phase diagram for a unary system, where a single pure substance is subject to a range of different temperatures and pressures. The fixed-point substance (the component) may exist in three different phases: solid, liquid, and vapour. According to the Gibbs' phase rule, such a system has f degrees of freedom,

$$f = c - p + 2, \quad (1)$$

where c is the number of components present, and p is the number of phases present. In one of the regions where a single phase exists ($p = 1$), the number of degrees of freedom is 2, so that the temperature and pressure may be varied independently. Along one of the three lines where two phases coexist (the freezing, boiling, or sublimation points), $p = 2$, there is a single degree of freedom, and once the pressure (or temperature) is fixed, the temperature (or pressure) is also fixed. Where three phases coexist in thermal equilibrium, the system has no degrees of freedom so the triple point occurs at a single temperature and pressure.

All four types of fixed points: freezing, boiling, sublimation, and triple points, are used for thermometry. However, the solid-liquid transitions (freezing or melting) and triple points are of particular interest because they exhibit a low or zero sensitivity to operating pressure. For all the phase-transition lines of Figure 1, the slope of the lines is given by

$$\frac{dT}{dP} = \frac{T\Delta V}{\Delta H}, \quad (2)$$

where P is the pressure, ΔV and ΔH are, respectively, the molar changes in volume and enthalpy at the transition temperature, T . Because the change in volume for a solid-liquid phase transition is normally very small, the sensitivity to pressure is also small, usually only a few millikelvin per atmosphere. The low sensitivity to pressure is also evident from the near-vertical line for the solid-liquid transition in the phase

diagram (Figure 1). For some fixed-point substances, including gallium and water, the volume decreases on melting so that the pressure sensitivity and the slope of the solid-liquid transition curve are also negative. Fixed points exhibiting a negative volume change are usually realised as melting points rather than freezing points to prevent liquid becoming trapped and pressurised within the solid, and causing an erratic freezing curve.

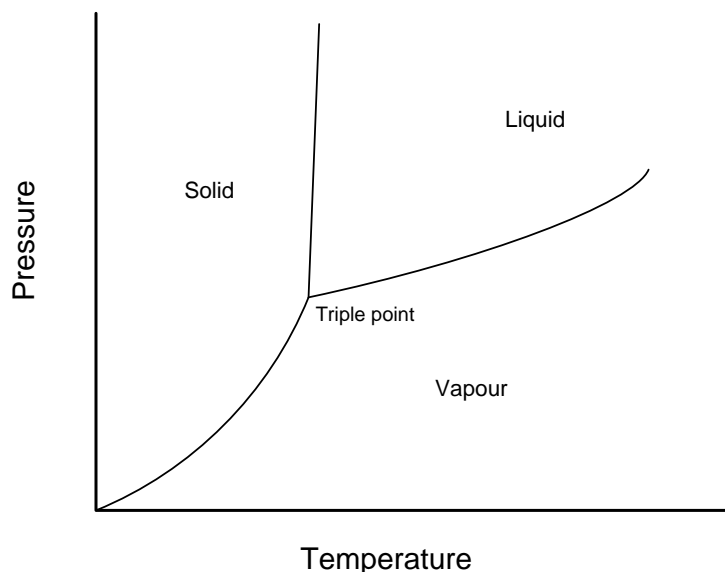


Figure 1. The P - T phase diagram for a unary system

If it is assumed that the vapour phases in liquid-vapour and solid-vapour transitions obey the ideal gas law, $PV = nRT$, where n is the number of moles of the gas, and R is the gas constant, Equation (2) can be integrated to yield

$$P = P_0 \exp \left[\frac{-\Delta H}{R} \left(\frac{1}{T} - \frac{1}{T_0} \right) \right], \quad (3)$$

which shows the exponential dependence of vapour pressure on temperature for both the boiling and sublimation transitions. Note that Equation (3) is an approximation due to the assumption of the ideal gas law, which is a good approximation only at very low gas densities, and also due to the assumption that ΔH is independent of temperature. Where boiling points and sublimation points are used as temperature references, more complex equations for the pressure-temperature relation are required.

2.2. Binary fixed points

When a second component is added to a system (i.e., two pure substances are mixed), Gibbs' phase rule, Equation (1), shows that the number of degrees of freedom increases by 1. This extra degree of freedom is often offset by assuming the effect of pressure is negligible by comparison to other sources of uncertainty, or by fixing the pressure to standard conditions. For temperature references, the standard pressure is the standard atmosphere, 101 325 Pa. However, for high-accuracy applications the pressure dependence should not be forgotten and it may need to be controlled or measured.

The assumption of fixed pressure means invariant points in phase diagrams continue to be found where three phases coexist (i.e., analogous to triple points). In binary systems, the invariant points are classified into at least eight different types [Massalski 1990]:

eutectic	$L \Leftrightarrow S_1 + S_2$
eutectoid	$S_1 \Leftrightarrow S_2 + S_3$
monotectic	$L_1 \Leftrightarrow S + L_2$
monotectoid	$S_1 \Leftrightarrow S_1 + S_2$
metatectic ¹	$S_1 \Leftrightarrow S_2 + L$
peritectic	$L + S_1 \Leftrightarrow S_2$
peritectoid	$S_1 + S_2 \Leftrightarrow S_3$
syntectic	$L_1 + L_2 \Leftrightarrow S$

where the reactions are written to indicate the direction of the reaction with cooling (warmer \Leftrightarrow cooler), L , L_1 , and L_2 denote distinct liquid phases, and S , S_1 , S_2 , S_3 denote distinct solid phases. Of these systems, eutectics are the most commonly used for secondary temperature references, but peritectic and eutectoid systems have also been investigated. Invariant reactions involving a liquid phase have the ending *-tectic*, while reactions occurring only within solid phases have the ending *-tectoid*. The phase diagrams for almost all possible binary systems have been collated in a large three-volume collection by Massalski [1990]. Some phase diagrams are also available online from proprietary databases.

2.2.1. Eutectics

Binary eutectics are formed from two different substances that are completely miscible in the liquid state but only partially miscible in solid state. The phase diagram of two substances, A and B, forming a simple binary eutectic is shown in

¹ Also called catatectic.

Figure 2. The horizontal axis shows the composition changing from pure A to pure B, and is commonly expressed as a percentage either by mass fraction or atomic fraction. The melting temperatures of the pure substances are T_A and T_B , respectively. Note that conventionally, the Greek symbols α , β , γ , ... are used in phase diagrams to indicate distinct solid phases with α being the leftmost in the phase diagram, β the next leftmost, etc. The point E indicates the eutectic point, at which three phases are in equilibrium. The three phases are the solid solution α , the solid solution β , and the liquid L . In equilibrium and at constant pressure, this invariant point defines the unique eutectic temperature T_E .

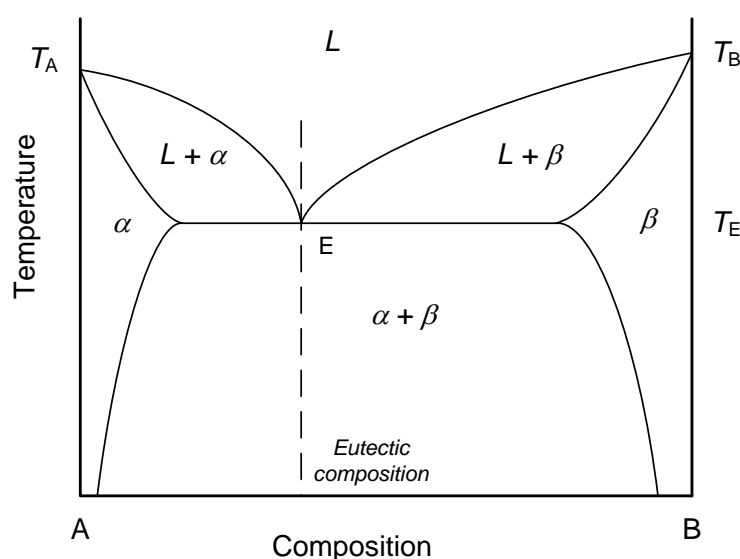


Figure 2. Binary phase diagram for a eutectic.

Each of the upper curves, describing the composition-dependent transition between liquid only and liquid + solid, is called the liquidus, and describes the temperature-composition relation for the onset of freezing as the mixture cools. The line between any of the liquid + solid regions and the purely solid-phase regions, α , β , and $\alpha + \beta$, is called the solidus, and describes the temperature-composition relation for the onset of melting as a sample warms. The lines between the different regions where only solid phases exist, e.g., between the α region and the $\alpha + \beta$ region, is called a solvus. Note the presence of the α and β solid solution regions indicated on the extreme left and right of Figure 2. In some systems, the solubility of the lesser fraction in the α or β phases may be so low that these regions are very narrow and practically invisible in the phase diagram, but the regions always exist and the precipitate from the liquid is never 100% pure. The α and β regions are often, incorrectly, omitted in some phase diagrams (see the discussion in Prince [1966, 74-75], and Naumann [2009, p223, p246]).

The eutectic reaction is one of the few invariant reactions that may characterise the complete behaviour of a binary system. More typically, the eutectic reaction

occurs within a more complicated collection of behaviours so that the phase diagram of Figure 2 may correspond to a subset of the larger diagram.

If a binary system has exactly the eutectic composition, it behaves much like a freezing point of a unary system, except that on solidification, two separate solids are formed: the α solid is mostly A with some B dissolved, and the β solid is mostly B with some A dissolved. When the eutectic reaction takes place, the two solids precipitate forming a complex microstructure with alternating regions of the α and β solids. The structures may be lamellar, globular, rod-like, or needle-like. During freezing, the components in the liquid must separate by diffusion to form the two different solid phases. Because the segregation and diffusion processes influence the local composition of the alloy, eutectic freezing temperatures and structures are very rate dependent, and often dependent upon the nucleation mechanism. In contrast, the melting point of a eutectic is more reproducible, and more so when the melt is preceded by a prolonged freeze allowing more time for the system to approach equilibrium conditions. For these reasons, the eutectic melting point is usually recommended as the reference temperature. Prolonged annealing of a binary-eutectic cell just below the eutectic temperature usually improves the quality of the subsequent melt. For metal-carbon systems, such anneals improve the duration and repeatability, and reduce the melt range of the fixed point [Woolliams *et al.* 2006, Machin 2013]. However, in the binary metal eutectics studied to date, annealing does not seem to have a significant effect [Ancsin 2008].

If the system does not have exactly the eutectic composition, liquidus occurs at a temperature above T_E and solid of either the α or β composition precipitates, depending on whether the composition is hypereutectic (right of E in the phase diagram) or hypoeutectic (left of E). The precipitation of only one of the solid phases causes the composition of the remaining liquid to move towards that of the eutectic. Therefore, as the precipitation progresses, the observed temperature falls towards the eutectic temperature. If the initial composition of the system is sufficiently close to the eutectic composition, a useful fraction of the freeze will occur at T_E . To maximise the duration of both the melts and freezes at the eutectic temperature, the composition should be close to the eutectic composition. Itoh [1983] found that changing the relative compositions by $\pm 2\%$ from the exact eutectic composition of the Cu-Ag system had no significant effect on the observed melting temperature. Metal-carbon eutectic systems are generally constructed with a hypoeutectic composition with the remaining graphite required to attain the eutectic composition being dissolved from the graphite crucible [Machin 2013].

The eutectic freezing temperature is rate-dependent and always lower than the melting temperature. Because the rate of freezing affects the slope of the subsequent melting curve [Bloembergen *et al* 2007], it is recommended that each melting-point determination is preceded by a slow freeze, if possible of several hours. Also, since even under optimum conditions the melting curve has a more pronounced slope than for a pure metal, some consistent criterion for choosing the melting temperature is required, and several methods have been suggested. McAllan [1982] suggested that the most reliable estimate for the equilibrium eutectic temperature of metal-metal eutectic systems is given by the intersection of the extrapolation of the region of the melting curve just before the commencement of the rapid rise with the 100%-melted

axis. Alternatively, the maximum in a histogram that shows percentage of time spent in consecutive temperature intervals can be taken as the melting temperature. An extension of this latter method, when the histogram has several peaks indicating segregation of impurities, is to use the centroid rather than the maximum. In principle, these last two methods give the same value, which is also the same as obtained by taking the point of inflection of the melting curve. The point-of-inflection definition has been shown to be particularly practical and reproducible for metal-carbon systems [Woolliams *et al.* 2006, Machin 2013].

The pressure dependence of eutectics is not well researched, but one study [Zhou *et al.* 1988] on metal-alloy eutectics indicated that the effect is well approximated by

$$\frac{dT_E}{dP} = \frac{T}{\Delta H_E} \sum x_i \Delta V_i, \quad (4)$$

where ΔH_E is the enthalpy for the eutectic reaction, x_i is the atomic fraction of the component, and ΔV_i are the molar volume changes for each component. For the Cd, Sn, and Pb alloys investigated, the pressure sensitivities were of the same order as the pure components; a few millikelvin per atmosphere.

2.2.2. Peritectics

The binary peritectic (Figure 3) has some similarities with the eutectic except that the peritectic temperature, T_p , lies between the melting points of the pure components A and B. As with the eutectic, the peritectic temperature occurs when three phases, α , β , and the liquid L, are in equilibrium, but unlike the eutectic, the transformation on cooling is from liquid plus the α phase to the β phase only.

Except for the region near to the pure component B, freezing starts with the formation of the solid α phase and the corresponding decrease of the concentration of component A in the liquid. Only once the peritectic temperature is reached, does the β phase form and the temperature stabilise. That is, the freeze plateau at T_p is preceded by a gradually falling liquidus temperature as the α phase forms. Once T_p is reached, a mixture of the phases L and α , which in combination have the peritectic composition, are transformed into the β phase. In principle, the temperature is stable so long as the transformation from $L+\alpha \Rightarrow \beta$ is incomplete. In practice, because the transformation takes place at the surface of the α phase, the β phase tends to entrap particles of the α phase and prevent them from further participating in the reaction [Prince 1966, Yamada *et al.* 2007, Naumann 2009]. For this reason, peritectic points should be run slowly to allow the components in the solid phase to diffuse and participate in the reaction. With close temperature control, and at higher temperatures where diffusion within the solid is greater, the plateaux of peritectic fixed points can be as useful as unary or eutectic fixed points.

At present, only few metal carbide-carbon peritectics have been investigated as secondary reference points. Early indications are that some of the melting points may be more repeatable than similar eutectic systems, with the WC-C peritectic at approximately 2748 °C being a particularly useful high-temperature fixed point

[Wang *et al.* 2013, Dong *et al.* 2013]. For the metal carbide-carbon peritectics, annealing does not appear to change the temperature or the range of a melt but it does significantly extend the duration of a melt [Zheng *et al.* 2008].

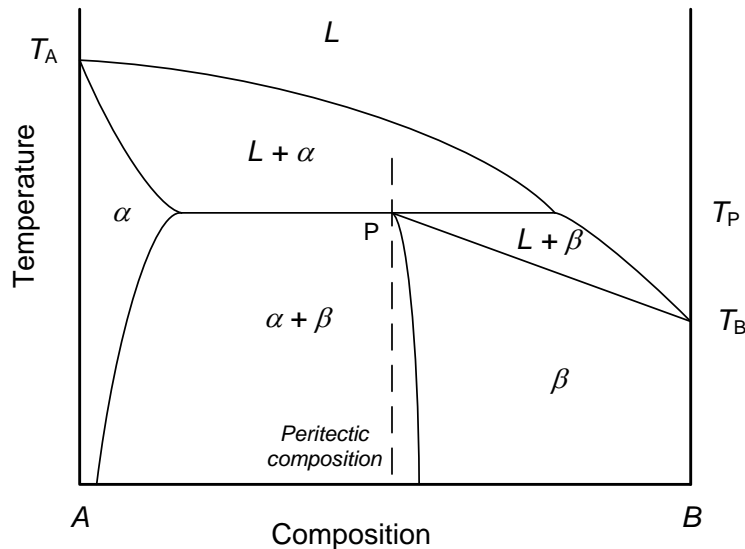


Figure 3. A simple binary peritectic phase diagram.

2.2.3. Eutectoids

Eutectoids are like eutectics except that the phase transition, $S_1 \Leftrightarrow S_2 + S_3$, occurs entirely within the solid. To date, two eutectoid systems have been investigated. The C-Fe eutectoid, which occurs with 0.76% carbon by mass at ~ 730 °C, was investigated by Yang and Kim [2007], and the Cu-Ge eutectoid, which occurs with 60% Cu at 614.7 °C which was investigated by Augustin *et al.* [2003].

Because the eutectoid reaction occurs only within solid, the eutectoid behaviour for the system is always a subset of the behaviour exhibited in a larger, more complicated phase diagram (see Figure 4) that must include, at least, additional liquid phases. For example, Augustin *et al.* [2003] exploited both the eutectoid (614.7 °C) and eutectic (642 °C) reactions within a single cell using a Cu-Ge alloy. There are several potential limitations with eutectoid systems that reduce the utility of these systems as fixed points. Firstly, the range of compositions for which the eutectoid reaction takes place might be narrow, e.g., only a few percent of the possible compositions. Secondly, the solid \Leftrightarrow solid aspect of the transition means that the latent heat is less than for a liquid \Leftrightarrow solid transition, and therefore the transition may be more difficult to exploit. Thirdly, because the reaction takes place entirely within a solid, it is highly dependent on diffusion within the solid, and such transitions may only be readily observable at high temperatures where diffusion is greater.

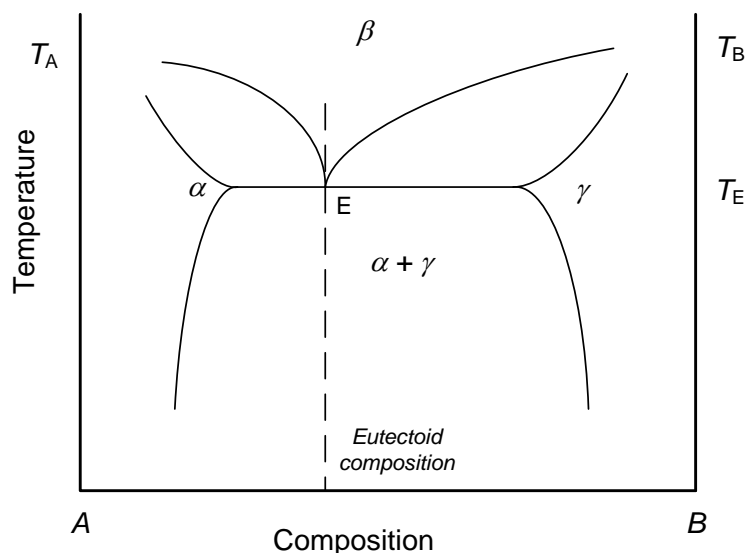


Figure 4. Simplified section of a phase diagram showing a eutectoid reaction.

3. Composition and temperatures for recently-investigated fixed points

The publication by Bedford *et al.* [1996] gives the most complete summary of the recommended values for a wide range of fixed points, including melting-point, freezing-point, triple-point, sublimation-point and boiling-point temperatures for a range of pure substances, as well as for a small number of eutectics. For guidance on the practical realisation of those points, the references cited by Bedford *et al.* should be consulted. Since the paper by Bedford *et al.* was published, there has been additional research leading to improved repeatability of some binary-metal eutectics, and a breakthrough in the use of metal-carbon systems for high-temperature applications. There have also been extensions to the ranges of pressure-temperature relations for fluids used in pressure-controlled heatpipes (boiling points). The following sections identify key references that report measurements of the phase transitions or provide advice on the realisations. These references are additional to those noted by Bedford *et al.* and should be read in conjunction with the previously cited references.

3.1. Liquid-vapour transitions

In recent decades, there has been increasing use of pressure-controlled heatpipes for calibration media [Merlone *et al.* 2003], with individual heatpipes able produce stabilities below 1 mK. In principle, according to Gibb's phase rule, knowledge of the pressure in these systems completely determines the temperature. In practice the repeatability's of these systems is not quite as good as for other fixed points. Recent evaluations of the pressure-temperature relations for several substances and their standard uncertainties ($k = 1$) are summarised in Table 1.

Table 1. Summary of recent investigations of selected liquid-vapour transitions

Substance	Temperature range	Uncertainty / K	References
Dodecane	190 °C to 260 °C	0.008	Renaot <i>et al.</i> [2003a, b]
Mercury	226 °C to 392 °C	<0.001	Merlone <i>et al.</i> [2010]
Caesium	370 °C to 660 °C	0.008	Hill and Gotoh [1996(a)]
Potassium	600 °C to 840 °C	0.011	Sadli <i>et al.</i> [1996] Renaot <i>et al.</i> [2003a]
Sodium	660 °C to 962 °C	0.012	Hill and Gotoh [1996(b)] Renaot <i>et al.</i> [2003a]

Mokdad *et al* [2012] describe a quasi-adiabatic calorimeter for the determination of the liquid-vapor pressure curve for water.

3.2. Triple points

Only one novel triple point has been recently investigated as a thermometric fixed point above 0 °C. Gotoh and Ode [2004] report that the triple point of iodine is 114.9 °C, with an uncertainty of about 0.1 °C.

3.3. Binary-metal systems

Two separate groups of binary-metal eutectics have been investigated, as summarised in Table 2. The first group includes gallium based eutectics investigated for near ambient applications, principally as small blackbody sources for medical or space-borne radiometric systems [Simpson *et al* 2008, Burdakin *et al* 2008]; the second group includes eutectics in the temperature range 500 °C to 800 °C, which were investigated to determine their suitability for the calibration of resistance thermometers and thermocouples [Augustin *et al.* 2003, Augustin and Boguhn 2003].

The melting point of the Cu-Ag eutectic (779.63 °C) was investigated extensively, because its melting temperature is well located in the 300 K interval between the freezing points of aluminium and silver; a strategically valuable temperature for both resistance and thermocouple thermometry. Studies of this eutectic point with resistance thermometers are described by Bongiovanni *et al.* [1972] and McAllan

[1982], with thermocouples by Itoh [1983], with optical pyrometers and thermocouples by Bedford and Ma [1982], and with an optical pyrometer by Jones and Tapping [1988]. Even when realized according to the same conventional procedures as for the pure metals according to ITS-90, the Cu-Ag eutectic was reproducible only within about 30 mK, in contrast to the reproducibility of 1 mK and less for pure metals. More recent measurements using a static adiabatic technique gave results with a repeatability of about 3 mK [Ancsin 2004]. Note too that the Cu-Ge alloy also exhibits a eutectoid reaction [Augustin *et al.* 2003].

Table 2. Summary of binary-metal phase transitions subject to recent investigation. Most of the phase transitions are eutectic reactions. The reported standard uncertainties ($k = 1$) are indicative only.

Composition (% by mass)	t_{90} / °C	u / K	References
Ga - In/20	15.648	0.002	Ivanova et al [2008]
	15.655	0.005	Burdakin <i>et al.</i> [2009]
Ga - Sn/13	20.482	0.0015	Ivanova [2004]
			Burdakin <i>et al.</i> [2009]
Ga - Zn/4	25.19	0.01	Burdakin <i>et al.</i> [2009]
			Ivanova et al [2009]
Ga - Al/1.67	26.95	0.03	Burdakin <i>et al.</i> [2009]
Cu - Sb/76.5	525.3	0.1	Augustin <i>et al.</i> [2003]
Al - Cu/33.1	548.16	0.025	Augustin <i>et al.</i> [2003]
			Ancsin [2007, 2008]
Ag - Al/29.5	567.72	0.025	Augustin <i>et al.</i> [2003], Ancsin [2008]
Al - Si/22.6	578.78	0.025	Augustin <i>et al.</i> [2003], Ancsin [2006]
Cu - Ge/29.6 ^(A)	614.7	0.1	Augustin <i>et al.</i> [2003]
Al - Pd/25.0	616.5	0.1	Augustin <i>et al.</i> [2003]
Al - In/17.3	638.4	0.1	Augustin <i>et al.</i> [2003]
Cu - Ge/29.6 ^(A)	642.4	0.1	Augustin <i>et al.</i> [2003]
Ag- Ge/18	652.4	0.1	Augustin <i>et al.</i> [2003]
Cu - Ag/71.7	779.64	0.005	Ancsin [2004]

^(A) Cu-Ge undergoes a eutectic reaction at 642.4 °C, and a eutectoid reaction at 614.7 °C.

3.4. Metal-carbon systems

A common problem with high-temperature fixed points is that the fixed-point substance may react with the crucible material and become contaminated. Yamada *et al.* [1999a, 1999b] recognised that this obstacle is overcome if the crucible material is a component of a binary system. The development of metal-carbon systems operating in graphite crucibles opens the possibility of a wide range of fixed points spanning temperatures from 1100 °C to 3200 °C. The range has been expanded to include metal-carbide-carbon systems and both eutectic and peritectic systems, as shown in Table 3, with the phase transitions at the higher temperatures being either metal-carbide-carbon eutectics or the WC-C peritectic.

The initial research into metal carbon systems was directed at eutectics for use in fixed-point blackbodies in radiation thermometry and radiometry. However, they rapidly became of interest for the calibration of high-temperature thermocouples. Because of the intense activity in recent years, the cited references in Table 3 tend to focus on reviews [Yamada *et al.* 2001, Sadli *et al.* 2004], and are not exhaustive.

Three of the metal-carbon eutectics, Co-C (~1324 °C), Pt-C (~1738 °C), and Re-C (~2475 °C), have exhibited very high reproducibility (below 0.1 °C) and are usefully spaced for multi-point calibrations, and these have been the subject of the greatest attention as reference points [Woolliams *et al.* 2016]. Note that some care is required when interpreting reports of temperature measurements for all the metal-carbon systems, especially at higher temperatures. Many will be ITS-90 temperatures, t_{90} , while other reported values may be thermodynamic temperatures, t .

4. Techniques for the calibration of contact thermometers

The fixed points used at temperatures above 0 °C are typically the freezing or melting points of pure metals or of eutectic alloys. The highest accuracy fixed points are the pure-metal freezing points defined by the ITS-90, typically realised in large graphite crucibles with two continuous liquid/solid interfaces surrounding the thermometer. The interface accompanying the solid on the outer wall of the crucible reduces the effects of thermal influences originating outside the crucible, while the inner interface accompanying the solid on the thermometer well determines the temperature measured by the thermometer. The techniques required in the generation of these interfaces, the crucible assemblies, furnace constructions, methods for checking the quality of the results, and uncertainties in the realisation of ITS-90 metal freezing points using sealed cells are described in detail in the *Guide to the Realization of the ITS-90* [Fellmuth *et al.* 2015, Pearce *et al.* 2015, McEvoy *et al.* 2015].

Table 3. Binary metal-carbon phase transitions. The temperatures t_{90} given are the ITS-90 temperature. The temperature values marked with (*) are thermodynamic temperatures t . All temperatures are for the point of inflection and are given with standard uncertainties $k = 1$. Accurate values of the temperature and uncertainties (u) of the transitions have been determined only for a subset of the systems.

Composition	Carbon/ %	Type	$t_{90} / ^\circ\text{C}$	u / K	References
Fe-C	4.2	Eutectic	1153		Yamada <i>et al.</i> [2001]
Co-C	2.6	Eutectic	1324.26*	0.07	Woolliams <i>et al.</i> [2016]
Ni-C	3.0	Eutectic	1329		Yamada <i>et al.</i> [2001]
Mn ₇ C ₃ -C	27	Peritectic	1330.72	0.2	Yamada <i>et al.</i> [2006]
Pd-C	2.7	Eutectic	1491.88*	0.13	Anhalt <i>et al.</i> [2006]
Rh-C	1.9	Eutectic	1657		Yamada <i>et al.</i> [2001]
Pt-C	1.2	Eutectic	1738.28*	0.09	Woolliams <i>et al.</i> [2016]
Cr ₇ C ₃ -Cr ₃ C ₂	37	Eutectic	1742.11	0.44	Pearce <i>et al.</i> [2014]
Si-SiC	0.7	Eutectic	1410.0	0.4	Suherlan <i>et al.</i> [2015]
Cr ₃ C ₂ -C	32.6	Peritectic	1826.15	0.4	Yamada <i>et al.</i> [2006] Yamada <i>et al.</i> [2007]
Ru-C	2.5	Eutectic	1953.98*	0.2	Anhalt <i>et al.</i> [2006]
Ir-C	1.6	Eutectic	2291		Sadli <i>et al.</i> [2004]
Re-C	2.0	Eutectic	2474.69*	0.18	Woolliams <i>et al.</i> [2016]
B ₄ C-C	31.1	Eutectic	2386		Woolliams <i>et al.</i> [2006]
(Mo _x C _{1-x})-C	9.3	Eutectic	2583		Sadli <i>et al.</i> [2004]
WC-C	41.5	Pertitectic	2747	0.5	Wang <i>et al.</i> [2013] Dong <i>et al.</i> [2013]
TiC-C	30	Eutectic	2760		Woolliams <i>et al.</i> [2006]
ZrC-C	20	Eutectic	2882		Sadli <i>et al.</i> [2004]
HfC-C	12.5	Eutectic	3185	1.3	Sadli <i>et al.</i> [2004]

Where less accurate fixed-point calibrations are required, the ITS-90 guidelines can be relaxed by easing the purity specifications of the fixed-point metal, or the size or geometry of the cell, or the presence or absence of gas-pressure control or measurement, or by using the fixed points differently. In this way, a wide variety of fixed-point techniques become available. Additionally, other fixed-point substances may be used. These include the unary metal fixed points: Bi, Cd, Pb, Sb, Au, Cu, Ni, Co, Ir, Pd, Pt and Rh, and a wide range of binary fixed point systems including binary-metal eutectics, metal-carbon eutectics, and metal-carbide-carbon systems.

The advent of metal-carbon systems has been the most significant development of recent years. At temperatures between 1100 °C and 1500 °C, these points have greatly simplified and reduced the uncertainty in calibrations of noble-metal thermocouples [Yamada *et al.* 2000, Edler *et al.* 2007, Morice *et al.* 2008, Pearce *et al.* 2008, Pearce and Machin 2008, Pearce *et al.* 2009]. Above 1500 °C, the techniques for realizing metal-carbon-eutectic fixed points become increasingly difficult, but successful use has been demonstrated at temperatures up to 2300 °C [Pearce *et al.* 2010, Pearce *et al.* 2013, Elliott *et al.* 2014].

For detailed information on the realisation of secondary reference points and uncertainty calculations, in the first instance consult the references cited here or by Bedford *et al.* [1996]. For metal-carbon eutectics, the review of Sadli *et al.* [2004] should be consulted. Because the realisations share some similarities with the ITS-90 fixed points, some of the contents of the *Guide to the Realization of the ITS-90* will be helpful. General information about measurement uncertainties can be found in *Evaluation of measurement data — Guide to the expression of uncertainty in measurement* [BIPM 2008] or in Nicholas and White [2001].

4.1. Sealed cells

The details of the internal construction of fixed-point cells vary according to the fixed-point, especially the chemical activity and transition temperature of the substance, and the furnace with which they are used. Figure 5 shows examples of the construction of large sealed and open fixed-point cells. The open cell on the right has the charged crucible within a fused-silica or glass tube. The tube also contains various layers of thermal insulation, thermal shunts, and radiation shields, all maintained under an inert gas such as high-purity argon. An additional fused-silica thermometer well extends from the gas-tight cell cap into the graphite thermometer well. The open cell conforms to the requirements of the ITS-90, but, in addition to a suitable furnace, requires an inert gas system accompanied by pressure control and measurement systems. In some circumstances, it may also be prone to contamination. The sealed cell, which is simpler to operate and may be more suitable for a less clean environment, is simply the charged crucible enclosed in a sealed fused-silica envelope filled with inert gas. In use, the sealed cell is placed in a more robust tube, often Inconel®, which contains all the insulation, shunts, radiation shields, and a thermometer guide tube.

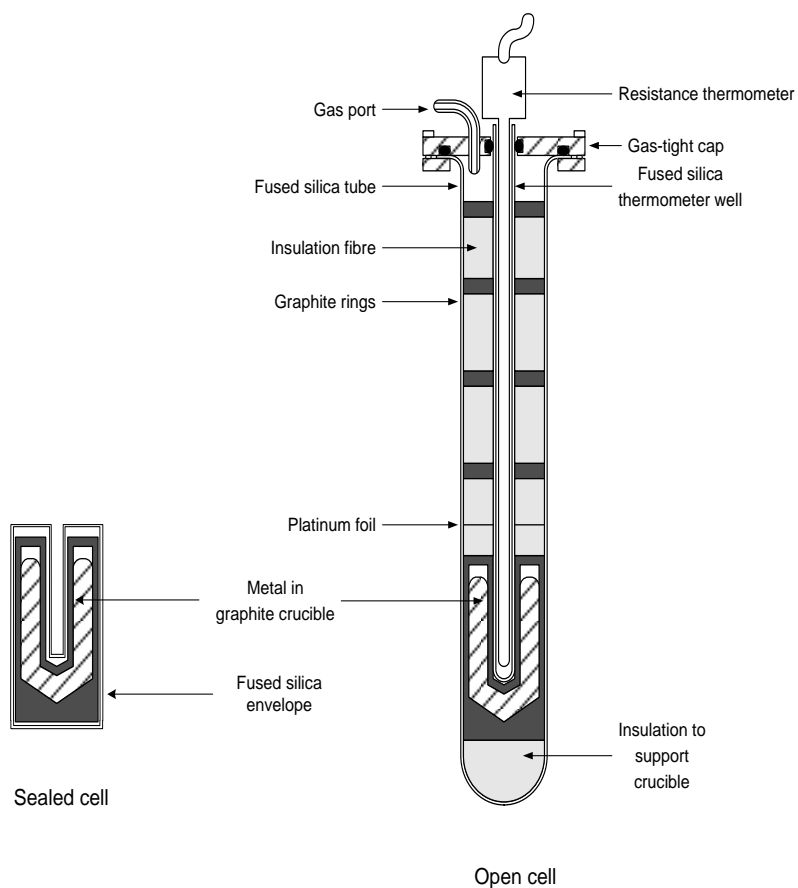


Figure 5. Simplified diagram showing the construction of metal fixed-point cells (not to scale) [Nicholas and White 2001]. Reproduced by permission of John Wiley & Sons.

The main disadvantage of the sealed cell is that the internal pressure, which should ideally be 101.325 kPa (1 atm.) at the fixed-point temperature, is not measurable in use. If the cells have been manufactured correctly, the internal pressure should be within a few percent of the standard pressure at the fixed-point temperature so that pressure errors are no more than a few hundred microkelvin. However, a significant fraction of sealed cells, especially those used at high temperatures (1 in 4 silver cells), have slow leaks in the envelope leading to realisations at an incorrect pressure and errors of up to 10 mK or more [White *et al.*, 2017]. For this reason, sealed cells have a lower status than open ITS-90 cells, a larger uncertainty in the realised temperature, and should be checked periodically against open cells.

4.2. Wire bridge and coil methods for thermocouples

The wire-bridge or wire-coil methods [Jahan and Ballico 2003], as illustrated in Figure 6, are often used to calibrate noble-metal thermocouples at temperatures above 1000 °C, most commonly at the gold (1064.18 °C), palladium (1554.8 °C), and platinum (1768 °C) melting points. The methods are simple, rapid, inexpensive, and adequately accurate. However, the methods have two main drawbacks. They cannot be applied to mineral-insulated metal-sheathed thermocouples, and, when calibrating reference thermocouples, it is necessary to remove the measuring junction and about 10 mm of the thermoelements and to re-weld the thermoelements after the calibration is complete, to avoid contamination. For these reasons, metal-carbon eutectic cells are usually preferred. No significant difference in the measured emfs has been found between the bridge and coil methods [Edler 2000].

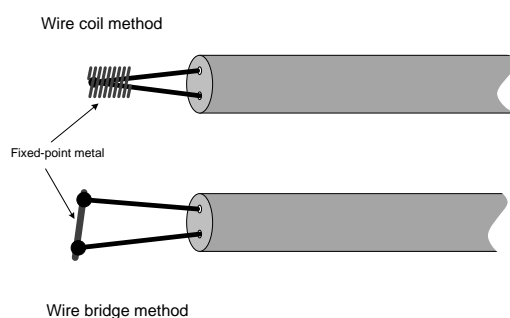


Figure 6. The wire coil and bridge methods for calibrating thermocouples.

With the coil version of the method, a small, ~0.1 g, piece of high-purity (at least 99.99 %) fixed point-metal in the form of 3 to 4 turns of wire (a small disk or rod may also be used) is crimped over the measuring junction of the thermocouple.

With the bridge technique, the piece of fixed-point metal is welded or clamped between the thermoelements. Welding is best carried out with a miniature hydrogen-oxygen gas torch to minimise contamination. Although the welding process alloys the fixed-point metal and thermoelements in the immediate vicinity of junctions between them, so long as the contaminated junction region is isothermal, there will be no thermoelectric error. Sometimes the wire bridge is wound as a small coil to relieve stress and prevent premature breakage during a melt, and this also minimises the effects of alloying and contamination caused by welding. To further avoid the risk of spurious emfs in the junction region, the wire bridge can also be clamped between the thermoelements. In either case, a pre-cleaning of the fixed-point metal in cool, dilute nitric acid is recommended.

To realise the fixed point, the thermocouple, with the wire bridge or coil, is slowly inserted into a furnace maintained several degrees below the melting point of the fixed-point metal. When thermal equilibrium is reached, the furnace power is slowly increased by a predetermined amount (0.2 K/min to 0.4 K/min yields suitable

melting plateaux [Kim *et al.* 1996]), and the thermocouple output is recorded as the temperature passes through the melting point. Occasionally, the metal bridge may break prematurely as melting starts, interrupting the thermocouple output. This is less of a problem with the wire coil method. During the melt, an increase in emf of a few microvolts is typical (smallest increase with Au, largest with Pt), with the melting lasting 2 to 8 minutes and with a momentary stabilization (0.5 min to 2 min) just before completion of melting. When melting is complete, the bridge often breaks, causing an open circuit condition. Which emf to assign to the fixed point is somewhat ambiguous. Bedford [1964] considered the value indicated before the sudden rise from the melting plateau to be the most reproducible value, whereas Crovini *et al.* [1987] recommend using the median of the plateau. It is advisable to test the reliability with a repeat calibration after clipping about 10 mm of the thermoelements from the measurement junction to avoid the effects of contamination.

Freezing points are not recommended with the wire-bridge or coil methods because the thermocouples may go open circuit during the preceding melt. Additionally, some material from the thermoelements usually dissolves in the molten bridge or coil, changing its freezing temperature by an indeterminate amount and producing a freezing transition with a changing temperature.

Some care is required when using the palladium point because the melting temperature is influenced by dissolved oxygen. In an oxygen-free atmosphere, the freezing temperature is recommended as 1554.8 °C [Bedford *et al.* 1996], based on measurements of Jones and Hall [1979], Coates *et al.* [1983], and Jones [1988]. However, the melting temperature in air is different. Figure 7 shows the dependence of the palladium melting temperature on oxygen partial pressure [Jones and Hall 1979]. The melting temperature follows Sievert's law and is about 1.5 K lower in air than in an oxygen-free atmosphere. Edler [2000] found a difference in the melting temperatures of Pd in pure argon and in air of 1.3 K by using miniature fixed points (see section 4.4) in alternating atmospheres during the melting processes itself.

The accuracy of a calibration procedure using wire methods is limited by the contamination of the fixed-point metals by the thermoelements and by the furnace's tendency to raise the temperature of the thermocouple legs, only weakly opposed by the latent heat absorbed by the melting bridge. With Type S thermocouples, it is possible to obtain a reproducibility ($k = 1$) of about $\pm 0.4 \mu\text{V}$ at the gold point [Kim *et al.* 1996], and of about $\pm 0.5 \mu\text{V}$ at the palladium point [Jahan and Ballico 2003]. A detailed description of the use of the wire-bridge method in an inter-laboratory comparison is given by Crovini *et al.* [1987].

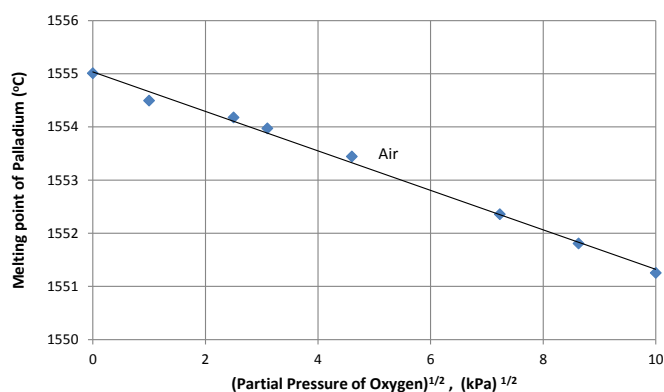


Figure 7. Dependence of the melting point of palladium on the partial pressure of oxygen [Jones and Hall 1979]. (The temperatures are based on the International Temperature Scale of 1968, IPTS-68). © Bureau International des Poids et Mesures. Reproduced by permission of IOP Publishing. All rights reserved.

4.3. Miniature cells

In 1982 Tischler and Koremblit [1982] developed a miniature fixed-point cell for thermocouple calibration, overcoming most of the disadvantages of the wire bridge and coil methods and yielding some of the advantages of regular fixed-point cells: lower uncertainties, neither the fixed-point substance nor the thermocouples become contaminated, the fixed-point substance is reusable, and the technique can be applied to thermocouples *in situ*. The cells were used successfully with In, Sn, Cd, Pb, Zn, Sb, Al, Ag, Au, and Cu using a small crucible (volume 0.1 cm³) machined from a 6 mm diameter graphite rod and filled with 0.2 g to 2 g of the pure metal, as shown in Figure 8(a). Holes were drilled through the graphite below the ingot chamber and another through the cell lid. In use, a thermoelement is inserted into each hole, and the graphite cell completes the electric circuit. The tightly fitted crucible lid has a small perforation to vent gases that are released as the temperature is raised and re-admit them on cooling.

A wide variety of different miniature cells have since been developed, examples of which are also shown in Figure 8. Ronsin *et al.* [1992] developed a larger miniature cell for an international comparison for calibration of Type S thermocouples (Figure 8(b)). The cell was made of a graphite cylinder about 65 mm long and 12.5 mm outside diameter, and contained about 15 g of pure silver. The cell was installed in a quartz glass tube filled with pure argon, which was long enough to allow the cell to be located close to the middle of the furnace. The thermocouple was introduced into the quartz glass tube through a small hole drilled in the silicone plug. The results of the comparison indicated agreement within 0.17 K between the calibrations of thermocouples in conventional large cells and in the miniature cells.

About the same time, Isothermal Technology (Isotech) manufactured a range of self-calibrating thermocouples with a separate layer of tin, zinc or gold encapsulating

the measurement junction [Ruppel 1992]. Similar designs were developed by Lehman *et al* [1996a, 1996b] and later by Augustin *et al* [2003] and Augustin and Boguhn [2003] who improved the thermal design of the assembly and used the technique to determine the melting temperature of binary alloys in the range 526 °C to 660 °C.

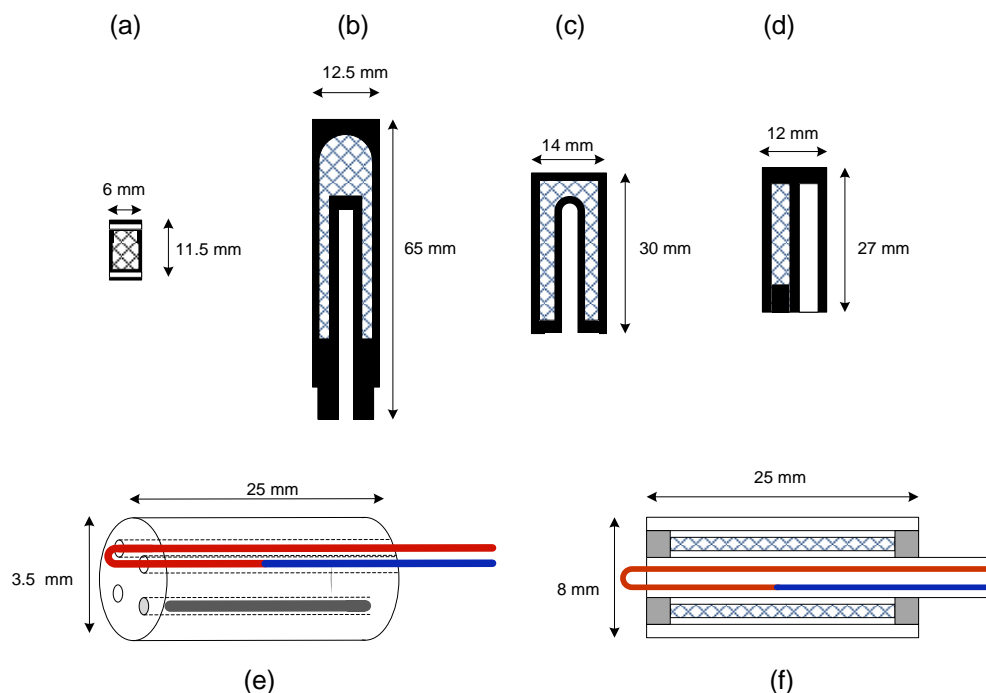


Figure 8. Miniature fixed-point cells for thermocouple calibration (see text for detail). The cells with graphite crucibles, (a), (b), (c), and (d) are drawn to the same scale for comparison.

Figures 8(c) and 8(d) show two recent examples of miniature cells [Failleau *et al* 2014]. The cell of Figure 8 (c) although only slightly larger than the cell of 8(d) contains about 7 times as much of the fixed-point substance, so produces longer and more repeatable melt and freeze plateaux (0.03 °C compared to 0.13 °C). The smaller cell is more robust against thermally induced stresses.

Figure 8(e) and 8(f) show two examples of miniature cells that are permanently fixed to noble-metal thermocouples [Mokdad *et al* 2015]. In Figure 8(e), the 'pulled wire' cell, the thermocouple is mounted in a 4-bore insulator with the end sections of the two spare bores filled and sealed with 25 mm lengths of the fixed-point wire. In Figure 8(f), the 'rolled wire' cell, fixed-point wire is wound around the thermocouple and covered by a 25 mm-long alumina sleeve that is sealed and cemented into place. In both Figure 8(e) and 8(f), the thermocouple junction is drawn down into one of the insulator bores so that it is adjacent to the fixed-point material. At the nickel melting point (1455.4 °C), the repeatability of the rolled wire cell was found to be about 0.1 °C, about 2 to 3 times better than of the pulled wire cell.

4.4. Freezing points of nickel and palladium in alumina crucibles

The freezing points of nickel (1455.4 °C) and palladium (1553.5 °C in air) are both useful for the calibration of thermocouples and have an uncertainty ($k = 1$) of about 0.2 °C [Kim *et al.* 2002, Edler 1997]. Because Ni and Pd react with graphite, the crucible is usually alumina ceramic rather than graphite. However, alumina ceramic is brittle and susceptible to thermal shock, and as crucible size increases, the risk of breakage increases. Great care is necessary, and rapid heating and cooling rates must be avoided.

Edler [1997] has investigated the melting point of Pd using different designs of miniature fixed-point cells made of pure alumina (Al_2O_3 , 99.7 %). About 0.4 g of Pd was filled into cell of Type I (Figure 9) with a length of 11 mm and a diameter of 4.5 mm. The measuring junction of the thermocouple was removed and the thermocouple wires were led along the crucible sides. The electrical connection between the thermocouple wires was made by a platinum shell, which wedged the wires to the outer wall of the crucible. The other type of cell (Type II) with a length of 17 mm and outer diameter of 11 mm corresponds to the classical form of fixed-point cells, with an inner re-entrant well to accommodate the measuring junction of a thermocouple. This type of cell was filled with a mass of about 1.2 g of Pd. Calibrations of Type B thermocouples have been performed a reproducibility ($k = 1$) of about 0.1 K.

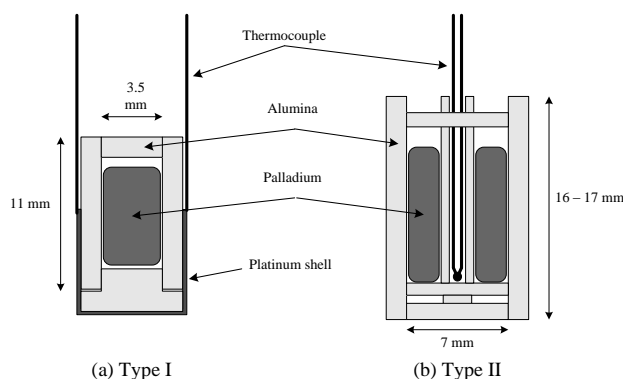


Figure 9. Schematic diagram of the miniature fixed points for the melting point of palladium [Edler 1997].

Successful realizations of the freezing points of Ni and Pd are also described by Kim *et al.* [1999, 2000, 2001]. The schematic design of a fixed-point cell and assembly is shown in Figure 10. All parts of the crucibles were made of alumina. The open end of the alumina protective tube (outer diameter 8 mm, inner diameter 5 mm) was fitted into the crucible cap to prevent the entrance of air through the protection tube. The tube was cut, fitted to the hole and cemented using a high temperature cement in region B. The other end, region A, was not fixed, so that the tube that protected the thermocouple could expand as the temperature increased, avoiding its breakage. High purity argon (99.999 %) was used to protect the metal from oxidation.

To realize the freezing points of Ni and Pd a dynamic freezing method was used. The melt was cooled at a constant rate until the supercool was observed. Then, on recalescence, the furnace temperature was set to 1 to 2 K below the freezing temperature. A reproducibility ($k = 1$) of less than $1 \mu\text{V}$ at the freezing point of Ni and of 1 to $2 \mu\text{V}$ at the freezing point of Pd was achieved with Type B thermocouples.

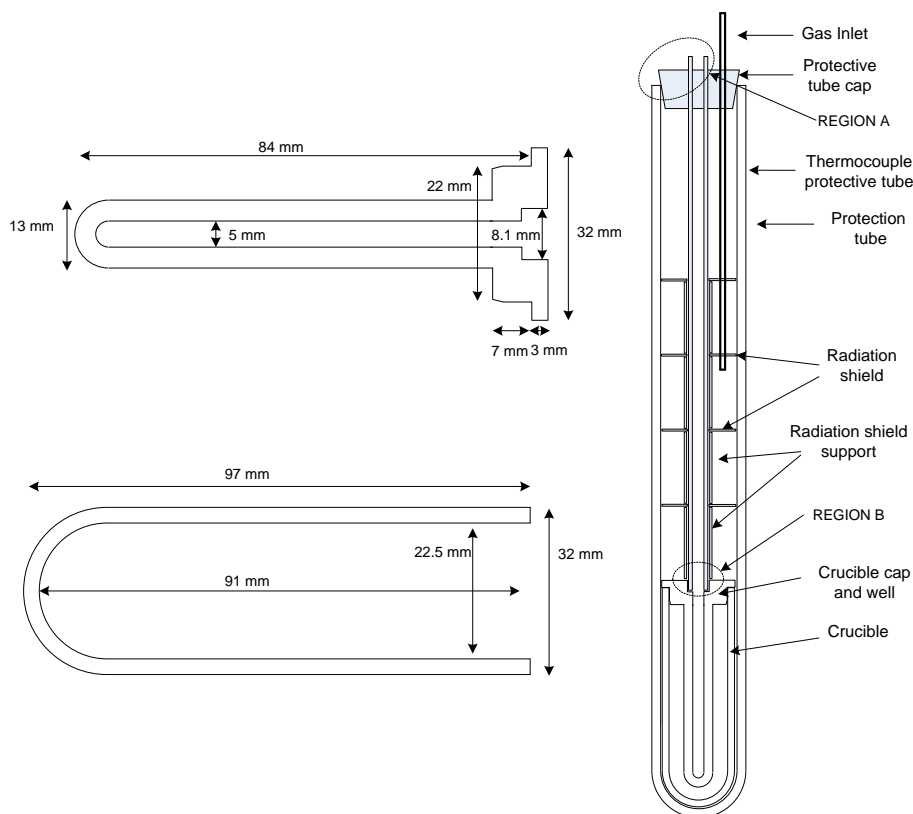


Figure 10. Schematic diagram of a Ni freezing point assembly, including details of the crucible and thermocouple well

Mokdad *et al* [2015] describe the application of the ‘pulled wire’ and ‘rolled wire’ thermocouple assemblies shown in Figure 8(e) and 8(f) to the realisation of the nickel and palladium points. These assemblies are much simpler and smaller than those of Figure 9 and 10, but because of the smaller quantities of fixed-point substance, the uncertainties in the realisations are larger, about $0.6 \text{ }^\circ\text{C}$ to $1.1 \text{ }^\circ\text{C}$ ($k = 1$).

4.5. Metal-carbon fixed-point cells for thermocouples

Yamada *et al.* [2000] were the first to propose and demonstrate the application of metal-carbon (M-C) fixed points (Section 3.4.), previously developed for radiation thermometry blackbodies, to the calibration of thermocouples. The advantage of M-C fixed points is that the carbon of the graphite crucibles is a component of the fixed-point material. Because graphite is available with high purities of 99.999%, the risk of contamination of the fixed-point material by impurities of the crucible material is minimized. The melting and freezing temperatures of M(C)-C eutectic alloys cover a

wide temperature range between 1154 °C (Fe-C) and 3185 °C (HfC-C), and a total of fifteen eutectic and three peritectic systems have been studied (see Table 3). For the calibration of contact thermometers above 1100 °C, the M-C eutectic fixed points are most often used. An exception is the $\text{Cr}_3\text{C}_2\text{-C}$ (1826 °C) peritectic point, which has been employed by Ogura *et al.* [2010] to calibrate W-Re thermocouples. A good overview of the development, construction and utilization of M-C eutectic fixed points can be found in Woolliams *et al* [2006] and Machin [2013].

A photograph and a schematic diagram of a fixed-point cell for M-C eutectics are shown in Figure 11. These are large cells consisting of a double-walled graphite cylinder with an axially symmetric thermometer well. The double-wall design minimizes the risk of failure of the M-C eutectic fixed-point cell during use. Often the fixed-point material bonds strongly to the inner walls, especially at rough edges of the crucible, and due to the different thermal expansion coefficients of the fixed-point materials and the graphite, the cells can break and fail. With the double-wall system, so long as there is a tight fit between the two walls, a broken cell can continue to be used as normal because the fixed-point material is contained and does not damage the outer wall. If cracks do become visible on the outer shell, it can be easily replaced.

The wall thickness of the thermometer well and the inner shell is typically between 2 mm and 4 mm, and the wall thickness of the outer shell is typically between 4 mm and 6 mm. The inner diameter of the thermometer well is typically between 8 mm and 12 mm allowing the calibration of contact thermometers of different diameters. The outer diameter of a double-walled cells ranges between about 30 mm and 46 mm. The length of eutectic fixed-point cells usable for the calibration of contact thermometers is typically 90 mm to 140 mm, although Ogura *et al* [2008] have also shown the application and the utility of longer cells (297 mm length).

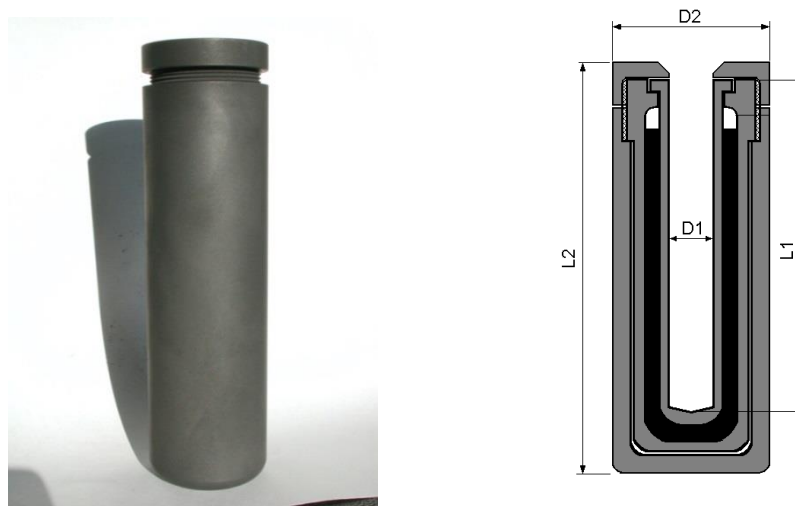


Figure 11. Photograph of a eutectic fixed-point cell and schematic diagram [Edler and Baratto 2006]. © Bureau International des Poids et Mesures. Reproduced by permission of IOP Publishing. All rights reserved.

The risk of breakage of M-C cells is much reduced for very small cells (up to 10 mm diameter, 20 mm long), and cells with a single, thin (1 mm) wall can be used reliably for thermocouple calibration *in-situ* [Pearce *et al.* 2010]. Ongrai *et al.* [2011], adapted some miniature cells, similar in construction to the cell of Figure 8(c), to high temperature metal-carbon eutectic fixed points (HTFPs), and to temperatures as high as the Co-C point (1324 °C). At higher temperatures, it was found that Pt thermocouple wire reacted adversely with the graphite. This led to further design modifications, and subsequently, the slightly larger mini-crucibles (Figure 8(c)) of eutectic material were successfully tested in conjunction with tantalum sheathed W/Re thermocouples to the Ir-C point (2292 °C) [Pearce *et al.* 2010, Pearce *et al.* 2013, Elliott *et al.* 2014, Machin *et al.* 2013, Machin 2013]. Further investigations have demonstrated the utility two different eutectics in a single cell [Ongrai *et al.* 2015], and proof of longevity after exposure *in situ* for periods of up to three months [Elliott *et al.* 2015].

M-C eutectic fixed points cannot be used in air. In general, a protective inert gas atmosphere of pure (at least 99.999 %) argon is used to realize the melting and freezing plateaus, and at any time when the fixed-point is above around 300 °C. Generally, the melting and freezing behaviour of M-C eutectics is different from that of conventional fixed points of pure metals. The inflection point of the melting curve is usually taken to represent the melting temperature of the corresponding M-C eutectic fixed point (see Section 2.2.1.) because of its very high reproducibility.

5. The ice point (0 °C)

The melting point of water is a very simple, effective and inexpensive temperature reference. As shown in Figure 12, the melting point of pure water at atmospheric pressure of 101325 Pa is near 0.0024 °C. However, this is not the ice point as it is used as a temperature reference. The practical ice point is the equilibrium temperature of ice and air-saturated water, which occurs at a pressure of 101.325 kPa at the lower temperature of 0.0 °C almost exactly. The 0.0024 °C difference is caused by dissolved air in the water and ice.

Historically the ice point was the defining point for many temperature scales until the more precise water triple-point cells were developed. It still has a major role in thermometry since it is a fixed point that can be readily achieved by almost any laboratory with a minimal cost. The main advantage of the ice point is that it can be made very simply and cheaply and, so long as the basic principles are followed [ASTM 2002, Nicholas and White 2001], it is relatively easy to achieve uncertainties of 10 mK, and with a little care it can be realised with an uncertainty of 1 mK, and with great care with an uncertainty of about 100 µK [Harvey *et al.* 2012].

Here we describe two methods for the realisation. The first, the free draining method, is the most accurate method but has a limited capacity to accommodate large amounts of heat being conducted along the stem or sheath of the thermometer. The second method, the slush method, has a greater heat absorption capability, but it is prone to errors of several millikelvin or more.

Thermoelectrically-operated ice-point devices are available for ease of use in less accurate thermometry, for instance, as reference junctions for thermocouples. Such

devices are particularly useful for long duration, unattended thermocouple measurements.

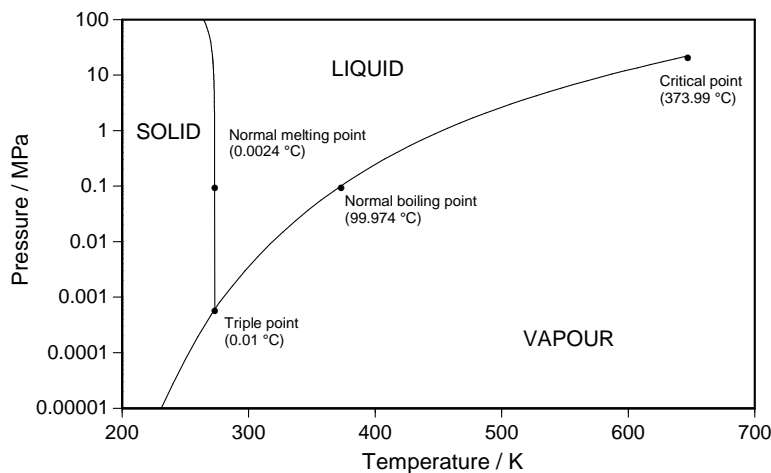


Figure 12. The phase diagram for water [Nicholas and White 2001]. Reproduced by permission of John Wiley & Sons.

5.1. The free-draining method

The preparation of an ice point requires the following equipment:

Flask: A thermally insulating container such as a vacuum-insulated flask or expanded polystyrene flask approximately 300 mm to 400 mm deep and 80 mm to 100 mm in diameter is ideal. It should be deep enough to hold the full length of the thermometer with about 50 mm extra depth to accumulate melt-water. If a metal-sheathed thermometer, such as a platinum resistance thermometer, is being checked, it will need to be immersed in the ice to a minimum of about 300 mm.

A siphon is placed in the flask, or the bottom of the flask is perforated, to enable the removal of excess water as the ice melts. Because the definition of the ice point is the equilibrium of melting ice and air-saturated water, air must be allowed to circulate through the melt water on the surface of the ice, especially if the water has been freshly distilled. In addition, water has its maximum density at about 4 °C. If a large volume of water is allowed to accumulate at the bottom of the flask, it is possible for the lowest layers of the water to become warm, and the ice to float on top. Ideally, the water level should not be allowed to rise to reach the sensing element of the thermometer.

Ice: Clean, shaved ice that is free of impurities and ideally made from distilled or de-ionised water is required. Because freezing is also a purification process for water, food-grade ice made in icemakers that employ a washing process is also satisfactory. Good, clean tap water is often satisfactory but should be avoided as it may

occasionally be contaminated or have a high concentration of additives from water treatment processes. If tap water must be used, check its electrical resistivity; at 10 °C its resistivity should be higher than $0.5 \times 10^6 \Omega\text{m}$. For high-accuracy applications, the quality of distilled water should also be checked as a poorly operated still can lead to impurity effects of several tenths of a millikelvin.

The ice must be shaved or crushed, ideally into small chips or snow measuring less than 1 mm across. For liquid-in-glass thermometers, which have a poor thermal conductivity, larger chips up to 5 mm will be satisfactory. However, for steel-sheathed thermometers, such as industrial platinum resistance thermometers, fine ice is essential if uncertainties below 0.01 °C are to be achieved. The ice may be shaved using commercial ice shavers ranging from low-cost hand-operated bar accessories to professional ice shavers. A good alternative, which is satisfactory for infrequent use, is a food processor with a grating disc. Note that discs with blades or knives are not suitable because they do not cut ice very effectively and the processor will be quickly damaged.

Water: Approximately 300 ml of clean water is required. Distilled water or de-ionised water is ideal, as is the melt water from the ice.

Rod: A clean rod of a similar diameter to the thermometer is used to make a hole in the ice.

The thermometer under test: The thermometer under test must be clean, and care should be taken not to contaminate the ice adjacent to the thermometer. Errors due to contamination of the ice can easily be several tens of millikelvin. If the thermometer is already clean it may be sufficient for it to be washed in distilled water and wiped dry with a clean cloth or tissue before insertion into the ice. Otherwise, cleaning with a solvent or light detergent may be necessary. If solvent or detergent is used, the thermometer must be rinsed thoroughly in distilled water and wiped dry before insertion into the ice.

The procedure: First, one-third fill the flask with clean water. Then fill the flask with the shaved ice. Freshly shaved ice is quite often colder than 0 °C, so wetting the ice ensures that it is melting. The difference in the condition of the ice is readily visible as cold ice freezes water vapour from the atmosphere giving it a white frosty appearance, like paper. By comparison the wet ice, at 0 °C, is translucent like waxed paper. The ice should always be transferred by using clean spoons or scoops and never touched by the hands.

For liquid-in-glass thermometers, the container should be filled to the top so that the thermometer can be immersed and the ice-point marking of the scale is visible just above the lip of the flask. The thermometer can then be read without parallax errors. For steel-sheathed thermometers of about 4 mm diameter, such as industrial platinum resistance thermometers or thermocouples, sufficient ice for about 300 mm immersion is required.

Siphon or drain off any excess water, and lightly compress the remaining ice to form a packed slush. This ensures good thermal contact while allowing the air and water on the surface of the ice to come to equilibrium.

Ideally the thermometer should be pre-cooled in ice before immersion into the ice point. For liquid-in-glass thermometers use the clean rod to make a hole

beforehand to prevent breakage and undue stress on the bulb. The sensing element must not go beyond the bottom of the ice where it can make thermal contact with the flask.

Once the thermometer is immersed, wait approximately 15 to 20 minutes for thermal equilibrium to be reached before reading the thermometer. Read the thermometer several times at intervals of a few minutes to be sure that equilibrium has been reached. For steel-sheathed resistance thermometers, it may be necessary to compress the ice quite firmly to achieve an uncertainty below 0.01 °C. Comparison with a second reading made at about 50 mm less immersion will indicate if there is any unwanted dependence on immersion depth.

A sheet of clean aluminium foil over the top of the ice can be used to prevent transmitted radiation from affecting the temperature of the sensing element. Contamination of the ice by the thermometer can be checked by withdrawing and immediately re-inserting the thermometer in a different location. Periodically it will be necessary to add ice to the top of the container and drain off the melt water to prevent the level rising to the bottom of the thermometer.

One of the largest sources of error is atmospheric pressure. Pressure differences accompanying differences in altitude change both the ambient pressure of the fixed point and the concentration of dissolved air in the water. Because the atmospheric pressure decreases exponentially with altitude the ice-point temperature is a non-linear function of altitude [Harvey *et al.* 2012]:

$$T = 273.16 - 0.01 \left[1 - 2.275 \times 10^{-5} h \right]^{5.256}, \quad (5)$$

where the temperature is in kelvin and the altitude, h , is in meters.

For altitudes below 5 km, Equation (5) is very nearly linear, and a correction of -1.0 mK/km is a good approximation. This corrects an error due to pressure alone of about 7.6 mK/101325 Pa, and an impurity error, due to reduced dissolved air, of about 2.4 mK/101325 Pa. Note that the ice-point temperature rises with increasing altitude.

5.2. The slush method

For the slush method, the procedure is very similar to that given above except that the water is left in the shaved ice to maximise the thermal contact between the ice and the thermometer. This makes the slush method more suitable for large-diameter metal thermometers. To achieve uncertainties below a few millikelvin, the slush must be well mixed and aerated, and there must be sufficient ice in the water to avoid having a layer of water containing no ice at the bottom of the container. The mixing and aeration can be carried out in a larger container beforehand if required. Once again, the sensing element of the thermometer should not be allowed to extend beyond the ice where it can make thermal contact with the wall, or be exposed to slightly warm water.

6. References

American Society for Testing and Materials (2002) *E563-02: Standard Practice for Preparation and Use of an Ice-Point Bath as a Reference Temperature* (ASTM, West Conshohocken)

Anhalt K, Hartmann J, Lowe D, Machin G, Sadli M, Yamada Y (2006) Thermodynamic temperature determinations of Co-C, Pd-C, Pt-C and Ru-C eutectic fixed-point cells, *Metrologia*, **43**, 78-83

Ancsin J (2004) A comparison of PRTs at the Cu-Ag eutectic point (780 °C), *Metrologia*, **41**, 198-203

Ancsin J (2006) Al-Si eutectic: A study of its melting and freezing behaviour, *Metrologia* **43**, 60-66

Ancsin J (2007) Al-Cu eutectic: An experimental study of its melting properties, *Metrologia* **44** (2007) 87-90

Ancsin J (2008) Manipulating the Melting behaviour of Metal-Metal Eutectics, *Int. J. Thermophys.* **29**, 181-189.

Augustin S, Bernhard F, Boguhn D, Donin A and Mammen H (2003) Industrially applicable fixed-point thermocouples, *Proc. TEMPMEKO 2001* (Ed. Fellmuth, Seidel & Scholz, VDE Verlag, Berlin) 3-8

Augustin S and Boguhn D (2003) Phase transformation temperatures of binary alloys in miniature fixed-point cells, *Proc. TEMPMEKO 2001* (Ed. Fellmuth, Seidel & Scholz, VDE Verlag, Berlin) 699-704

Bedford R E (1964) Reference Tables for Platinum 20% Rhodium/Platinum 5% Rhodium Thermocouples, *Rev. Sci. Inst.* **35**, 1177-1190

Bedford R E, Bonnier G, Mass H and Pavese F (1996) Recommended values of temperature on the International Temperature Scale of 1990 for a selected set of secondary reference points, *Metrologia*, **33**, 133-154 (Available at <http://www.bipm.org/en/committees/cc/cct/publications-cc.html>)

Bedford R E and Ma C K (1982) Measurement of the melting temperature of the Copper 71.9 % Silver eutectic alloy with a monochromatic optical pyrometer, In *Temperature: Its Measurement and Control in Science and Industry*, Vol. 5 (Ed. J F Schooley, AIP, New York) 361-369

BIPM, Bureau International des Poids et Mesures (2008) *Evaluation of measurement data – Guide to the expression of uncertainty*, JCGM 100:2008 (Available at <http://www.bipm.org/en/publications/guides/gum.html>)

Bloembergen P, Yamada Y, Sasajima N, Wang Y and Wang T (2007) The effect of the eutectic structure and the residual effect of impurities on the uncertainty in the eutectic temperatures of Fe-C and Co-C. *Metrologia*, **44**, 279-293

Bongiovanni G, Crovini L and Marcarino P (1972) Freezing and melting of silver-copper eutectic alloys at very slow rates, *High Temp.- High Press.*, **4**, 573-587

Burdakin A, Khlevnoy B, Samoylov M, Sapritsky V, Ogarev S, Panfilov A, Bingham G, Privalsky V, Tansock J, Humpherys T (2008) Melting points of gallium and of binary eutectics with gallium realized in small cells, *Metrologia* **45** 75–82

- Burdakin A, Khlevnoy B, Samoylov M, Sapritsky V, Ogarev S, Panfilov A, Prokhorenko S (2009) Development of Gallium and Gallium-Based Small-Size Eutectic Melting Fixed points for Calibration procedures on Autonomous Platforms, *Int. J. Thermophys.*, **30**, 20-35
- Coates P B, Chandler T R D and Andrews J W (1983) A New Determination of the Freezing Point of Palladium, *High Temp.-High Press.*, **15**, 573-582.
- Crovini L, Perissi R, Andrews J W, Brooks C, Neubert W, Bloembergen P, Voyer G and Wessel I (1987) Intercomparison of Platinum Thermocouple Calibration, *High Temp.-High Press.*, **19**, 179-194
- Dong W, Lowe D H, Lu X, Machin G, Yuan Z, Wang T, Bloembergen P, Xiao C (2013) Bilateral ITS-90 Comparison at WC-C Peritectic Fixed Point Between NIM and NPL, in *Temperature: Its Measurement and Control in Science and Industry, Vol. 8* (AIP, New York) pp. 786-790
- Eidler F (2000) *Rauschthermometrische Bestimmung der thermodynamischen Temperatur des Palladiumschmelzpunktes mit Hilfe miniaturisierter Fixpunktzellen* (dissertation.de) ISBN 3-89825-056-3
- Eidler F and Baratto A C (2006) Comparison of nickel-carbon and iron-carbon eutectic fixed point cells for the calibration of thermocouples, *Metrologia*, **43**, 501-507
- Eidler F, Ederer P, Baratto A C, and Viera H D (2007) Melting Temperatures of Eutectic Fixed-Point Cells Usable for the Calibration of Contact Thermometers, *Int. J. Thermophys.*, **28**, 1983-1992
- Eidler F (1997) Miniature fixed points at the melting point of palladium, *Proc. TEMPMEKO 1996* (Ed. P Marcarino, Levrotto & Bella, Torino) 183-188
- Elliott C, Pearce P, Machin G, Schwarz C, Lindner R (2012) Self-validating thermocouples for assured temperature measurement confidence and extended useful life, in *Proc. 12th European Conference on Spacecraft structures, materials and environmental testing, ESA Communications* (Ed. I Ouwehand, ESA) ISBN 978-92-9092-255-1
- Elliott C, Failleau G Deuzé, T, Sadli M, Pearce J, Machin G (2014) Long-term Monitoring of Thermocouple Stability with Miniature Fixed-Point Cells, *Int. J. Thermophys.*, **35**, 560-573
- Failleau G, Elliott CJ, Deuzé T, Pearce JV, Machin G and Sadli M (2014) Miniature Fixed-Point Cell Approaches for In Situ Monitoring of Thermocouple Stability. *Int. J. Thermophys.* **35**, 1223-1238.
- Fellmuth B, Hill K D, Pearce J V, Peruzzi A, Steur P P M, Zhang J (2015) *Guide to the Realisation of ITS-90: Fixed points: Influence of impurities* (BIPM, Available at <http://www.bipm.org/en/committees/cc/cct/publications-cc.html>)
- Gotoh M and Ode J (2004) Fabrication of the Iodine Triple -Point Cell, *Proc TEMPMEKO 2004* (Ed. D Zvizdic, University of Zagreb, Zagreb) 257-260

- Harvey A H, McLinden M O, and Tew W L (2013) Thermodynamic Analysis and Experimental Study of the Effect of Atmospheric Pressure on the Ice Point, In *Temperature: Its Measurement and Control in Science and Industry*, Vol. 8 AIP Conf. Series 1552 (Ed. C Meyer, AIP, New York) 221-226
- Hill K D and Gotoh M (1996a) The vapour pressure of caesium between 370 °C and 660 °C, *Metrologia*, **33**, 307-317
- Hill K D and Gotoh M (1996b) The vapour pressure of sodium between 660 °C and 962 °C, *Metrologia*, **33**, 49-60
- Itoh H (1983) The Ag-Cu eutectic point as a reference temperature (in Japanese), *Trans. Soc. Inst. Cont. Eng.*, **19**, 978-982
- Ivanova A, Gerasimov S, Elgourdou M, Renaot E (2004) The Peculiarities of Phase Transitions of Ga-Sn Alloys, *Proc. TEMPMEKO 2004* (Ed. D Zvizdic, University of Zagreb, Zagreb) 267-270
- Ivanova A G, Gerasimov S F (2008) Fixed point on the basis of Ga-In eutectic alloy for rapid monitoring of thermometers and temperature measurement systems, *Meas. Tech.* **51** 498-502
- Ivanova A G, Gerasimov S F (2009) The dependence of the phase transition temperature of Ga-Zn eutectic alloy on its morphology, *Meas. Tech.* **52** 52-56
- Jahan F and Ballico M (2003) The mini-coil method for calibration of thermocouples at the palladium point, In *Temperature: Its Measurement and Control in Science and Industry*, Vol. 7 AIP Conf. Series 1552 (Ed D C Ripple, AIP, New York) 523-528
- Jones T P and Tapping J (1988) The determination of the thermodynamic temperature of thermometry fixed points in the range 660 °C to 1064 °C, *Metrologia*, **25**, 41-47
- Jones T P (1988) The Freezing Point of Palladium in Argon, *Metrologia*, **25**, 191-192
- Jones T P and Hall K G (1979) The Melting Point of Palladium and Its Dependence on Oxygen, *Metrologia*, **15** 161-163.
- Kim Y-G, Kang K H and Gam K S (1996) Reproducibility of the gold melting point of the Type S thermocouple by the wire-bridge method with change of the heating rate, *Measurement*, **17**, 45-49
- Kim Y-G, Park S N, Gam K S and Kang K H (2002) Realization of the nickel freezing point for the thermocouple calibration, *Proc. TEMPMEKO 2001* (Ed. Fellmuth, Seidel & Scholz, VDE Verlag, Berlin) 495-500
- Kim Y-G, Gam K S and Kang K H (1999) Realization of the palladium freezing point for thermocouple calibrations, *Metrologia*, **36**, 465-472
- Kim Y-G, Gam K S and Kang K H (2000) Fabrication of a nickel freezing-point cell and preliminary study of its behaviour, *Metrologia*, **37**, 243-245
- Kim Y-G, Gam K S, and Kang K H (2001) A nickel freezing-point cell for thermocouple calibration, *Metrologia*, **38**, 319-323
- Lehmann H and Bernhard F (1996a) Self-Calibrating Thermocouples Part 1: Modelling, design of Prototypes Proc. TEMPMEKO 1996 Ed P. Marcarino, (Levrotto and Bella, Torino) 195-200

- Lehmann H and Bernhard F (1996b) Self-Calibrating Thermocouples Part 2: Modelling, design of Prototypes Proc. TEMPMEKO 1996 Ed P. Marcarino, (Levrotto and Bella, Torino) 201-206
- Machin, G (2013) Twelve years of high temperature fixed point research: a review, AIP Conf. Proc. 1552, 305-316
- Machin G, Anhalt K, Edler F, Pearce J, Sadli M, Strnad R, Veulban E, (2013) HiTeMS: A project to solve high temperature measurement problems in industry, *AIP Conf. Proc.* 1552, 958.
- McAllan J V (1982) Reference temperatures near 800 °C, In *Temperature: Its Measurement and Control in Science and Industry*, Vol. 5 (Ed. J.F. Schooley, AIP, New York) 371-376
- McEvoy H, Machin G, Montag V (2015) Guide to the Realisation of ITS-90: Fixed points for Radiation Thermometry (BIPM, Available at <http://www.bipm.org/en/committees/cc/cct/publications-cc.html>)
- Massalski T B, Okamoto H, Subramanian P R, and Kacprzak L (1990) *Binary alloy phase diagrams*, 2nd ed., (ASM International, Materials Park, Ohio)
- Merlone A, Musacchio C (2010) The mercury vapour pressure vs. temperature relation between 500 K and 665 K, *The Journal of Chemical Thermodynamics*, Volume 42, Issue 1, Pages 38-47
- Merlone A, Dematteis R, Marcarino P (2003) Gas-Controlled Heat Pipes for Accurate Liquid-Vapour Transition Measurements, *Int. J. Thermophys.*, **24**, 695-712
- Mokdad S, Georgin E, Hermier Y, Sparasci F, and Himbert M, (2012) Development of a quasi-adiabatic calorimeter for the determination of the water vapor pressure curve *Rev. Sci. Inst.* **83**, 075114
- Mokdad S, Failleau G, Deuzé T, Briauveau S, Kozlova O and Sadli M (2015) A Self-Validation Method for High-Temperature Thermocouples Under Oxidizing Atmospheres. *Int. J. Thermophys.*, **36**1895-1908
- Morice R, Edler F, Pearce J, Machin G, Fischer J, Filtz J R (2008) High-temperature fixed-point facilities for improved thermocouple calibration – Euromet project 857, *Int. J. Thermophys.*, **29**, 231-240
- Naumann R J (2009) *Introduction to the Physics and Chemistry of Materials* (CRC Press, Taylor and Francis, Boca Raton)
- Nicholas J V and White D R (2001) *Traceable Temperatures: An Introduction to Temperature Measurement and Calibration* (John Wiley and Sons, Chichester).
- Ogura H, Izuchi M, Arai A (2008), *Int. J. Thermophys.* 29, 210-221
- Ogura H, Deuze T, Morice R, Ridoux P, Filtz J R (2010) Construction of a Cr₃C₂-C peritectic point cell for thermocouple calibration, *SICE JCMSI*, **3**, 2, 81-85
- Ongrai O, Pearce J V, Machin G, and Sweeney S J (2011) A miniature high-temperature fixed point for self-validation of type C thermocouples. *Meas. Sci. and Technol.* 22 105103

- Ongrai O, Pearce JV, Machin G and Norranim U (2015) Multi-Mini-Eutectic Fixed-Point Cell for Type C Thermocouple Self-Calibration. *Int. J. Thermophys.* **36**, 423-432
- Pearce J V, Machin G, Ford T, Wardle S, (2008) Optimising heat-treatment of gas turbine blades with a Co-C fixed-point for improved in-service thermocouples, *Int. J. Thermophys.*, **29**, 222-230
- Pearce J and Machin G (2008) A robust Pd-C fixed point for the calibration of thermocouples, *Acta Metrologica, Sinica*, **29**, 5A, 224-228
- Pearce J V, Ogura H, Izuchi M, Machin G, (2009) Evaluation of the Pd-C eutectic fixed point and the Pt/Pd thermocouple, *Metrologia*, **46**, 473-479
- Pearce J V, Ongrai O, Machin G, and Sweeney S J (2010) Self-validating thermocouples based on high temperature fixed points, *Metrologia*, **47**, L1-L3
- Pearce J V, Elliott C J, Machin G, Ongrai O (2013) Self-validating type C thermocouples to 2300 °C using high temperature fixed points, *AIP Conf. Proc.* **1552**, 595-600
- Pearce J V, Elliott C J, Lowe D H, Failleau G, Deuzé T, Bourson F, Sadli M, Machin G (2014) Performance of Pt–C, Cr₇C₃–Cr₃C₂, Cr₃C₂–C, and Ru–C Fixed Points for Thermocouple Calibrations Above 1600 °C, *Int J Thermophys.*, **35**, 547-559
- Pearce J V, Steur P P M, Joung W, Sparasci F, Strouse G, Tamba J, Kalemci M (2015) Guide to the Realisation of ITS-90: Metal Fixed Points for Contact Thermometry (BIMP, Available at <http://www.bipm.org/en/committees/cc/cct/publications-cc.html>)
- Preston-Thomas H, (1990) The International Temperature Scale of 1990, *Metrologia*, **27**, 3-10, also erratum: *Metrologia*, **27**, 107. (The full text of the amended version of ITS-90 is available at http://www.bipm.fr/en/committees/cc/cct/publications_cc.html).
- Prince A (1966) *Alloy Phase Equilibria*, Elsevier, Amsterdam
(on-line copy at <http://www.msiport.com/msi-research/free-tools/a-prince-alloy-phase-equilibria/>)
- Renaot E, Elgourdou M, Bonnier G (2003a) The “Temperature Amplifier”: An Innovative Application of Pressure-Controlled Heat-pipes for Calibration of PRTs and Thermocouples, in *Temperature: Its measurement and Control in Science and Industry* Vol 7 (Ed D C Ripple, AIP, New York) 939-944
- Renaot E, Favreau J O, Elgourdou M, Bonnier G (2003b) Thermal Characteristics of a Dodecane Heat-pipe over the Range from 190 to 260 °C and Related Impurity Effects, in *Temperature: Its measurement and Control in Science and Industry*, Vol 7 (Ed D C Ripple, AIP, New York) 945-949
- Ronsin H, Elgourdou M, Bonnier G, Chattle M V, Read S J, Bongiovanni G, Perrisi R, Wessel I, Groot M J and Dekker R (1992) Assessment of mini-crucible fixed points for thermocouple calibration, through an international comparison, *Temperature: Its Measurement and Control in Science and Industry*, Vol. 6 (Ed. J.F.Schooley, AIP, New York) 1061-1066

- Ruppel FR (1991) Evaluation of the self-calibrating thermocouple as a front end to a smart temperature measurement system in *Temperature: Its Measurement and Control in Science and Industry, Vol. 6* (Ed. J.F.Schooley, AIP, New York) 637-642
- Sadli M, Renaot E, Elgourdou M, Bonnier G (1996) Approximation of the ITS-90 Between 600 °C and 830 °C using the Potassium Vapour P-T relation, *Proc. TEMPMEKO 1996* (Ed. P Marcarino, Levrotto and Bella, Torino) 49-54
- Sadli M, Fischer J, Yamada Y, Sapritsky V I, Lowe D, and Machin G (2004) Review of metal-carbon eutectic temperatures: proposal for new ITS-90 secondary points, *Proc. TEMPMEKO 2004* (Ed D Zvizdic, University of Zagreb, Zagreb) 341-347
- Simpson R, McEvoy H C, Machin G, Howell K, Naeem M, Plassmann P, Ring F, Campbell P, Song C, Tavener J, Ridley I (2008) In field-of-view thermal image calibration system for medical thermography applications, *Int. J. Thermophys.*, **29**, 1123-1130
- Suherlan, Kim Y-G, Joung W, Yang I (2015) Temperature determination of the Si-SiC eutectic fixed point using thermocouples, *Metrologia*, **52**, 330-336
- Tischler M and Koremblit M J (1982) Miniature Thermometric Fixed Points for Thermocouple Calibrations, In *Temperature: Its Measurement and Control in Science and Industry Vol. 5* (Ed. J F Schooley, AIP, New York) 383-390
- Wang T, Sasajima N, Yamada Y, Bai C, Yuan Z, Dong W, Ara C and Lu X (2013) Realization of the WC-C peritectic fixed point at NIM and NMIJ, in *Temperature: Its Measurement and Control in Science and Industry, Vol. 8* AIP Conf. Series 1552 (AIP, New York) 791-796
- White D R, Fellmuth B, Hill K, Ivanova A, Peruzzi A, Rusby R, Strouse G (2017) Uncertainties in the realisation of ITS-90 metal freezing points using sealed cells. CCT Working document CCT/17-20
<http://www.bipm.org/cc/CCT/Allowed/28/Report-TG-SMFPC-2017-20.pdf>
- Woolliams E R, Machin G, Lowe D and Winkler R (2006) Metal(carbide)-carbon eutectics for thermometry and radiometry: a review of the first years, *Metrologia*, **43**, R11-R25
- Woolliams E R, Anhalt K, Ballico M, Bloembergen P, Bourson F, Briaudeau S, Campos, J, Cox MG, Del Campo D, Dong W and Dury MR (2016), Thermodynamic temperature assignment to the point of inflection of the melting curve of high-temperature fixed points, *Phil. Trans. R. Soc. A*, **374**: 2015.0044
- Yamada Y, Sakate H, Sakuma F and Ono A (1999a) Radiometric observation of melting and freezing plateaus for a series of metal-carbon eutectic points in the range 1330 °C to 1950 °C, *Metrologia*, **36**, 207-209
- Yamada Y, Sakate H, Sakuma F, and Ono A (1999b) A possibility of practical high-temperature fixed points above the copper point, *Proc. TEMPMEKO 1999*, (Ed. J F Dubbeldam and M J de Groot, NMi Van Swinden Laboratorium, Delft) 535-540
- Yamada Y, Sakuma F, Ono A (2000) Thermocouple observations of melting and freezing plateaus for metal carbon eutectics between the copper and palladium points, *Metrologia*, **37**, 71-73

Yamada Y, Sakate H, Sakuma F and Ono A (2001) High-temperature fixed points in the range 1150 °C to 2500 °C using metal-carbon eutectics, *Metrologia* **38**, 213-219

Yamada Y, Wang Y, Sasajima N (2006) Metal-carbide-carbon peritectic systems as high-temperature fixed points in thermometry, *Metrologia*, **43**, L23-L27

Yamada Y, Wang Y, Zheng W, Sasajima N (2007) A Study of the Metal carbide-Carbon Peritectic Phase Transition for the Cr-C System, *Int. J. Thermophys.*, **28**, 2028-2040

Zheng W, Yamada Y, Wang Y, (2008) Experimental investigation of the Cr₃C₂-C peritectic fixed point, *Int. J. Thermophys.*, **29**, 935-943

Zhou W, Shen Z-Y, Yin X-J, Zhang Y, Zhao M (1988), Effects of pressure on the eutectic or eutectoid temperatures of the Cd-Pb, Cd-Sn, Pb-Sn and Cd-Pb-Sn systems, *J. Less Common Metals*, **143**, 59-69